Ninth International Conference on CFD in the Minerals and Process Industries
CSIRO, Melbourne, Australia
10-12 December 2012

Numerical Simulation of the Collision of a Droplet with a Heated Solid Surface

Monica GUMULYA[1], Ranjeet P. UTIKAR[1], Vishnu PAREEK[1], Moses O. TADE[1] and Geoffrey M. EVANS[2]

[1] Department of Chemical Engineering, Curtin University of Technology, WA, AUSTRALIA
[2] School of Engineering, University of Newcastle, NSW, AUSTRALIA
*Corresponding author, E-mail address: r.utikar@curtin.edu.au

ABSTRACT

This paper discusses the development of a model for the evaporation of a droplet on heated solid surface. Associated issues include the construction of evaporative source terms, and their implementation into a multiphase (VOF) framework. This was done in conjunction with the Level Set method (CLSVOF), allowing the evaporation at the liquid-vapour and liquid-solid interface to be characterised accurately.

The validity of the model was examined through comparisons with published experimental data. The model was found to be capable of reproducing the reduced droplet spreading rate as the surface temperature is increased away from the saturation temperature. This decrease in surface wetting results from the combined effects of surface tension, viscous forces and contact line evaporation. The effects of increased pressure due to evaporation, which in some cases can be quite severe such that the liquid gets lifted-off from the surface, were also captured, in good agreement with experimental observations.

NOMENCLATURE

C_P heat capacity
$\mathbf{f}_{ST}$ momentum source term due to surface tension
$\mathbf{g}$ momentum source term due to gravity
$\dot{h}$ enthalpy source term
h_{lv} enthalpy of vaporisation
N Normalisation factors
p pressure
S_i area of liquid-vapour interface in cell
t time
T temperature
$\mathbf{u}$ velocity
V_i cell volume

α volume fraction
ε distance parameter
λ thermal conductivity
μ viscosity
ρ density
φ mass evaporation rate
Φ level set function

Subscripts
l liquid
v vapour
i interface

INTRODUCTION

Many commercially important catalytic processes, such as fluid catalytic cracking (FCC) and olefin polymerization, etc., involve the interaction of fluid droplets with heated solids. These interactions are complex in nature, with a myriad of possible contact modes, as well as heat and mass transfer characteristics (Chandra and Avedisian, 1991). These intricacies make the modelling of such systems challenging, and requires various simplifications and assumptions regarding the operating conditions and the characteristics of heat and mass transfer within the system (Berry et al., 2004; Nayak et al., 2005).

While the problem of interaction between falling droplets and solid surfaces has been extensively studied (Sazhin, 2006), the additional complexity that results from the coupling of heat and mass transfers causes various aspects of the phenomenon to remain unclear. The dynamic interaction between the droplet and solid surfaces is dependent on a number of factors, namely the size and velocity of the droplets, the volatility of the liquid, surface tension and contact angles, as well as the temperature and heat capacity of the solid surface. The dependence of the droplet dynamics on these factors, which are generally difficult to control experimentally, as well as the small spatial and temporal scale of the problem, have made it difficult to obtain appropriate experimental data. As a result, detailed CFD models are required, such that the effects of these factors on the dynamics and evaporation of the droplets upon contact with solid particles could be evaluated.

MODEL DESCRIPTION

Governing equations

A numerical model based on the volume-of-fluid (VOF) method has been developed, incorporating equations for mass, momentum, and heat transfer for both liquid and vapour phases. Source terms have been included in the mass, heat, and volume-fraction equations, to account for the evaporation of the liquid phase:

$$\nabla \cdot (\rho \mathbf{u}) = \dot{\rho} \tag{1}$$

$$\frac{\partial \rho \mathbf{u}}{\partial t} + \nabla \cdot (\mathbf{u} \cdot \rho \mathbf{u}) = -\nabla p + \nabla \cdot (\mu \cdot \nabla \mathbf{u}) + \mathbf{f}_{ST} + \mathbf{g} \tag{2}$$

$$\frac{\partial \rho C_p T}{\partial t} + \nabla \cdot \left(\mathbf{u} \cdot \rho C_p T\right) = \nabla \cdot \left(\lambda \cdot \nabla T\right) + \dot{h} \quad (3)$$

$$\frac{\partial \rho \alpha}{\partial t} + \nabla \cdot \left(\mathbf{u} \cdot \rho \alpha\right) = \dot{\rho} \alpha \quad (4)$$

where the volume fraction parameter (α) represents the volume fraction of the liquid phase in each computational cell. An α value of 1.0 represents a cell that is completely filled with the liquid phase, whereas 0.0 the opposite. At each control volume the density of the mixture was calculated as follows:

$$\rho = \alpha \rho_l + \left(1 - \alpha\right) \rho_v \quad (5)$$

The viscosity and thermal conductivity of the mixture were computed in a similar manner. The parameter of thermal conductivity was calculated as follows:

$$\lambda = \alpha \frac{C_{Pl} \mu_l}{\mathrm{Pr}_l} + \left(1 - \alpha\right) \frac{C_{Pv} \mu_v}{\mathrm{Pr}_v} \quad (6)$$

The temperature gradients at the liquid-vapour interface and local vaporisation rates were calculated using the Level Set parameter (Φ), which is analogous to the volume fraction parameter, α. The former parameter gives a sharper definition of the liquid-vapour interface, in contrast to the VOF-based α field which tends to place the interface over several computational cells, unless rigorous interface reconstruction schemes are employed. At each time step an initial guess of Φ was calculated based on the α field:

$$\Phi = \left(2\alpha - 1\right)\varepsilon \quad (7)$$

where ε is a distance parameter. The value of Φ is therefore 0 at the interface, $+\varepsilon$ in the liquid phase, and $-\varepsilon$ in the vapour phase. This initial estimate was then corrected using the approach of Sussman and Puckett (2000):

$$\frac{\partial \Phi}{\partial \tau} = sign\left(\Phi_0\right)\left(1 - \left|\nabla \Phi\right|\right) \quad (8)$$

where τ is a pseudo time parameter and $sign(\Phi_0)$ is the numerically smeared-out sign function.

Source terms for droplet evaporation

The local evaporation rate at the interface was determined as follows:

$$\varphi_{0,i} = \frac{\lambda_l \left(T_i - T_{sat}\right) S_i}{h_{lv} \Phi V_i} \quad (9)$$

Equation (9) was applied in cells surrounding the liquid-vapour interface, such that problems associated with the zero value of Φ at the interface could be avoided. The sharpness of interface provided by the level set function enables the stable implementation of this calculation method.

Evaporation also occurs in cells that are completely filled with the liquid phase. The local evaporation rate for this type of evaporation was thus calculated as follows:

$$\varphi_0 = \frac{\rho_l C_{pl} \left(T_i - T_{sat}\right)}{h_{lv} \Delta t} \quad (\text{for } \alpha = 1.0) \quad (10)$$

The total local evaporation rate, φ_0, is thus the sum of equations 9 and 10.

The approach of Hardt and Wondra [2008] was used to obtain a continuum-field representation of the evaporation rates:

$$\dot{\rho} = N_v \left(1 - \alpha\right)\varphi - N_l \alpha \varphi \quad (11)$$

where N_v and N_l are normalisation factors to ensure that mass that disappears, reappears on the other side of the interface; and φ is a diffusively smeared version of φ_0, calculated through an inhomogeneous Helmholtz equation.

The developed model was implemented in the OpenFOAM (Open Source Field Operation and Manipulation) CFD package.

Initial and boundary conditions

At time t = 0, a liquid droplet (1.5 mm diameter) is positioned at 0.9 mm above a heated solid surface. The initial temperature field in the domain is set to 24°C, whereas the bottom surface is set to several different temperatures (24, 100, 150, 180°C). No slip boundary conditions are set on all the walls and the tendency for the liquid wetting on the bottom surface is described by a contact angle parameter, which was set to be a function of surface temperature in accordance to the experimental findings of Chandra and Avedisian (1991).

RESULTS

A series of test cases was selected based on the experimental data of Chandra and Avedisian (1991), involving an n-heptane droplet with an initial diameter of 1.50 mm. The droplet hits a solid surface with an impact velocity of 0.93 m/s. Several different surface temperatures were tested: 24°C, 100°C, 150°C, 175°C, and 180°C. These temperatures are below the Leidenfrost temperature of n-heptane (≈ 200°C), and therefore the dynamics of the droplets are expected to reflect this selection. The ambient temperature was held constant at 24°C. The contact angle between the n-heptane fluid with the solid surface was set according to the experimental data published by Chandra and Avedisian (1991). The value of this variable was found to be a function of the surface temperature, ranging from 32° to 180°.

All calculations were conducted on a two-dimensional uniform axisymmetric grid. The resolution of this grid will be discussed further in the following section. The time step of the calculation was set such that the maximum Courant number was kept below 0.1.

Grid Independence

An assessment of the convergence and stability of the current numerical method was conducted through a series of simulations on numerical grids with 4 different resolutions: 70, 90, 180, and 210 cells per droplet diameter (cpd). The solid surface temperature for this analysis was set to 150°C.

The dynamics of the droplet was characterised by the extent of its spread on the solid surface (d). The spread factor β (=d/D), as a function of time elapsed since the droplet hits the heated surface is shown in Figure 1. The droplet shows tendency to spread after colliding with the heated surface, forming a circular film of a finite height (h). Once a maximum value of β is reached, the circular

film tends to decrease in diameter and retract. Figure 1 shows that the simulation with lowest spatial resolution (70 cpd) tends to over-estimate the spreading rate of the droplet. Similarly, upon retraction, simulations with lower grid resolutions tend to under-estimate the retraction rates of the droplet (cf. 70 and 90 cpd with 180 and 210 cpd). The similarities in the droplet spreading and retraction dynamics of the 180 and 210 cpd simulations indicate that a grid-independent solution has been achieved with a grid resolution of 180 cpd.

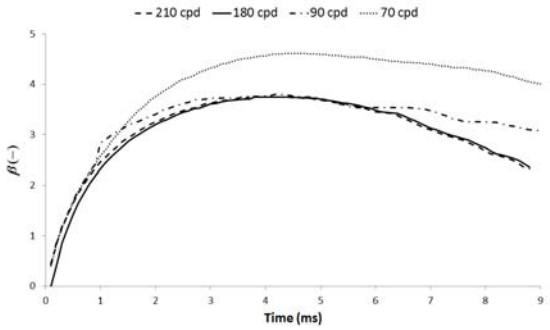

Figure 1: The spread factor (β) of a n-heptane droplet on a 150°C solid surface, as a function of the grid resolution.

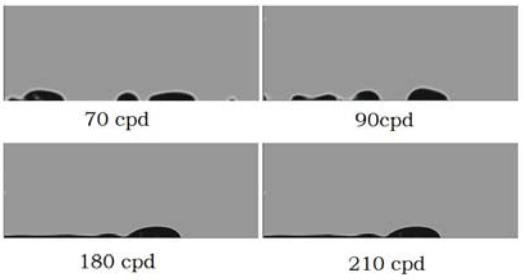

Figure 2: Comparison of the spread of a n-heptane droplet on a 150°C solid surface, 6ms after it reaches the surface.

As the liquid spreads, a wave-like structure is formed at the outer edge of the circular film, due to the surface tension and contact angle effects of the fluid on the solid surface. The shape of this wave can be seen in Figure 2, where it is evident in the simulations of 180 and 210 cpd resolutions. At resolutions of 70 and 90 cpd, the thinnest part of the film (~ 0.05 mm according to the results of the 180 cpd simulation) was less than 3 computational cells in thickness, thus introducing considerable error towards the reconstruction of the α field. This is evident in Figure 2, where the profiles of the droplets in the 70 and 90 cpd simulations are markedly different from those resulting from the higher-resolution simulations. This large error in the α field is believed to cause the marked difference in the retraction dynamics of the films as seen in Figure 1. The grid independence of the numerical method is therefore dependent on the minimum thickness of the droplet as it spreads across the heated surface.

Similar results were obtained with all the other surface temperatures analysed in this study. Grid resolution of 180 cpd was therefore used for all of the subsequent simulations.

Qualitative assessment

The results of the simulations for a solid surface temperature of 24°C are given in Figure 3. The profiles suggest that the numerical model was able to closely replicate the spreading dynamics of the droplet as that observed by Chandra and Avedisian (1991). As the droplet hits the surface (impact velocity of 0.93 m/s), the rapid increase in pressure in the bottom layer of the droplet causes it to jet out sideways from the point of impact, thus spreading the droplet into a circular film. This continues to occur until the dissipated pressure cannot overcome the viscous effects at the liquid-solid interface, upon which the film starts retracting.

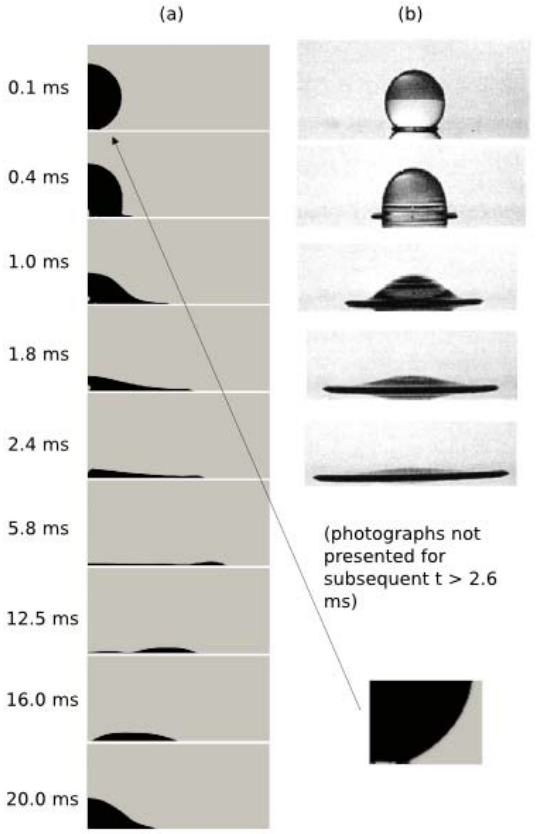

Figure 3: Spread of a n-heptane droplet on a 24°C surface: (a) simulation result, (b) Chandra & Avedisian (1991). The inset shows the air cavity formed at the bottom of the droplet as it impacts with the solid surface.

At t < 1.8 ms, a single bubble could be seen that the centre of the droplet. The presence of this bubble has been attributed towards the formation of a small cavity of air formed at the bottom of the liquid during the impact process, as evident in the inset of Figure 3. As the film continues to spread and decrease in thickness, the bubble starts to rise to the surface of the film, eventually disappearing at t = 2.4 ms.

The rest of the simulation results are presented in Figures 4-5, where it can be seen that the shape of the droplet changes considerably with surface temperature. In Figure

4(a) (T_w = 100°C), it can be seen that the higher surface temperature causes a higher population of bubbles to appear in the spreading liquid. At t = 3.8 ms, it can be seen that most of the larger bubbles have risen to the surface and collapsed. Smaller bubbles may still exist in the liquid phase at this stage; however they could not be detected with the current level of numerical resolution. With the progression of the simulation, more liquid evaporates, and the size of the bubbles increases. This can be seen in Figure 4(a) at t = 25 and 30 ms.

Furthermore, as the evaporation occurs mainly at the solid-liquid contact line, it is expected that the fluid spreads to a lower value of β_{max}. A higher rate of retraction could also be expected, as the outer layer of liquid evaporates away from the surface. The figures in Figure 4(a) are consistent with this hypothesis.

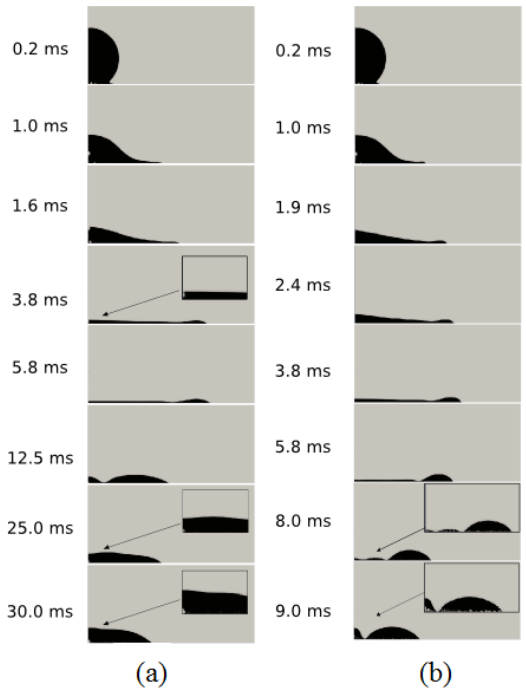

Figure 4: The spread of a n-heptane droplet: (a) on a 100°C surface, (b) on a 150°C surface. The insets show the details of the liquid profile.

Interestingly, the figures in Figure 4(b) suggest that there is a lower population of bubbles in the spreading liquid in the case of T_w = 150°C than in cases with lower surface temperatures. The bubbles caused by air entrapment during impact rise to the surface of the film and collapse at t = 1.6 ms, similar with the case of T_w = 100°C (cf. T = 2.4 ms for T_w = 24°C). Beyond this time frame, however, the liquid phase appears to spread without any bubble entrapment (see t = 2.4, 3.8, and 5.8 ms in Figure 4(b)). This observation is contradictory to the results of Chandra and Avedisian (1991), who reported the presence of micro-bubbles throughout the liquid phase, caused by heterogeneous nucleation. This discrepancy could be caused by the size of the micro-bubbles, which at this stage are too small to be sufficiently resolved with the current level of numerical resolution. As the evaporation continues at the interface, the size of the bubbles increases, and their presence becomes much more evident in the simulation results (e.g. t > 8 ms). The presence of nucleation sites and micro-bubbles was also not evident in the cases of T_w = 175 and 180°C, until the later stages of the simulations, where the size of the bubbles becomes sufficiently large to be captured at the current level of numerical resolution (t ~ 6 and t ~ 5 ms for T_w = 175°C and 180°C, respectively). This apparent increase in the rate of bubble-growth could thus be attributed towards the increase in the rate of evaporation, as the surface temperature deviates further from the saturation temperature.

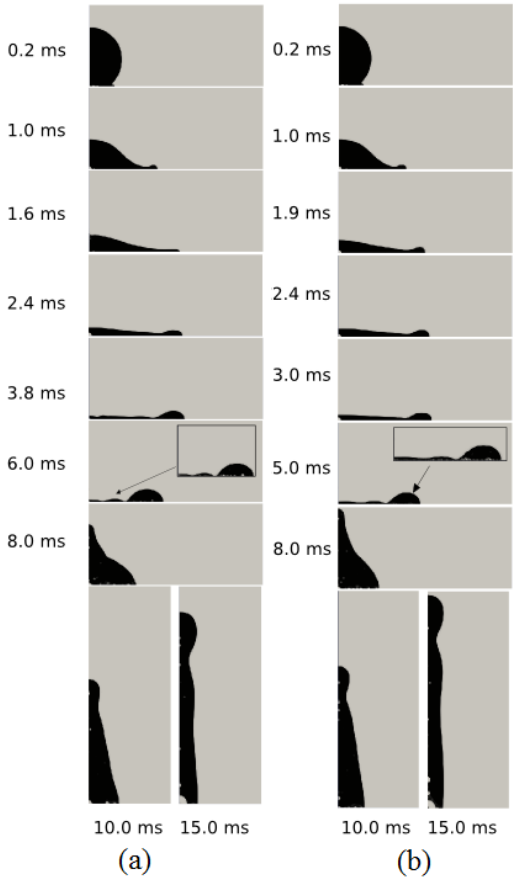

Figure 5: The spread of a n-heptane droplet: (a) on a 175°C surface, (b) on a 180°C surface. The insets show the details of the liquid profile.

In Figure 5 (a) and (b), it can be seen that with the progression of the simulations, there are some instances where the droplets tend to rise away from the solid surface. In the case of T_w = 175°C, the droplet could be seen to be partially lifted from the surface, creating separate packets of liquid, which then fall back to the surface and recoil. At T_w = 180°C, the droplet is almost completely lifted away from the surface, before recoiling back in a similar manner to the case with T_w = 175°C. This phenomenon has been attributed towards the rapidity of the evaporation process, which generates vapour of sufficient pressure at the droplet-solid contact line to lift

the liquid away from the bottom surface. This finding was found to be similar to the observations of Chandra and Avedisian (1991).

Spreading rate

To further compare the results of the simulation with the experimental results of Chandra and Avedisian (1991), the variability of β with time for 4 different experimental configurations (T_w = 24, 100, 150, and 180°C) has been presented graphically in Figure 6. As the spread of the droplet is highly dependent on both the dynamics of the liquid and vapour phases and the boundary conditions of the temperature field, an apparent agreement on the variability of this parameter would strongly indicate the validity of the current numerical model.

In Figure 6, it can be seen that at $t < 0.5$ ms the rate of spread of the droplet is almost independent of surface temperature. This is as expected, as the motion of the fluid at this stage is dominated by the internal pressure resulting from its collision with the solid surface. As the droplet continues to spread, the surface tension and viscous effects of the fluid become more dominant. Eventually, a maximum spread factor (β_{max}) is reached, and the fluid recoils back. The value of β_{max}, as it can be seen in Figure 4, tends to decrease with increasing value of T_w. This is as expected, due to the evaporation of the liquid phase at the contact line at temperatures above the saturation temperature of the liquid.

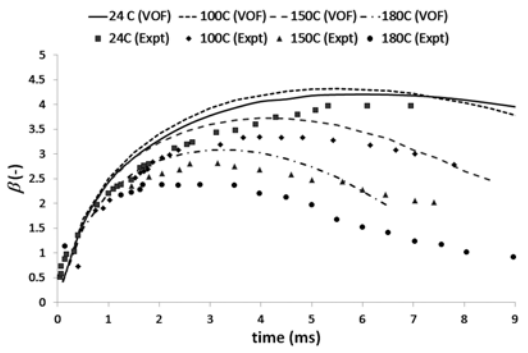

Figure 6: The spread factor (β) of a n-heptane droplet on a 24, 100, 150, and 180°C solid surface. The hollow markers denote the results of Chandra and Avedisian (1991).

DISCUSSION

A closer inspection of Figure 6 reveals the simulations tend to over-estimate the spreading rate of the droplet in comparison to the experimental data of Chandra and Avedisian (1991). This was found to be especially true in cases where T_w was well above the saturation temperature. Furthermore, the results of Chandra and Avedisian (1991) also indicate that the droplet tends to retract earlier than that predicted through the simulations.

The discrepancy in the droplet spreading rates could be caused by the errors introduced by the contact angle parameter, which at this stage has been assumed to be a function of surface temperature only. To closely reproduce these experimental results, the effects of the fluid velocity at the contact line need to be characterised. Furthermore, it has to be noted that the parameters of contact angle presented by Chandra and Avedisian (1991) were in actuality measured properties of the advancing (i.e. spreading) liquid film. Closer inspection is therefore required to further characterise the properties of the receding (i.e. retracting) liquid film.

The differences in the simulation and experimental results could also result from the use of an axisymmetric grid to discretise the governing equations. Future studies on this subject will be conducted to examine the effects of this discretisation method on the dynamics of the droplet. Nevertheless, Figure 4 shows an apparent agreement in the trend of β as a function of both t and Tw. This adequate agreement with the experimental data suggests the validity of the numerical model presented.

SUMMARY

A numerical model based on the VOF method has been developed with the aim of characterising the dynamics and evaporation of a droplet upon impact with a heated solid surface. Special consideration was given towards the implementation of the evaporation source term into the VOF calculation. The implementation of the Level Set method (CLSVOF) was found to facilitate the precise reconstruction of the vapour-liquid interface, such that exact temperature gradients and local vaporisation rates could be determined.

The resulting numerical model was found to have good agreement with the experimental data of Chandra and Avedisian (1991), especially the dynamics of an n-heptane droplet falling on a 24°C surface. As the droplet hits the surface, a rapid increase in pressure in the bottom layer of the droplet causes the liquid to jet out sideways from the point of impact, spreading it into a circular film. This occurs until the dissipated pressure cannot overcome the viscous effects at the liquid-solid interface, causing the liquid to retract. With higher temperatures ($T_w \geq 98.4$°C), the numerical model was found to be able to reproduce the decrease in the spreading rate of the liquid due to evaporation, as well as the effects of pressure increase at the bottom layer of the liquid due to evaporation. At 175°C and 180°C, it was found that this increase in pressure was sufficient to partially lift the liquid from the solid surface, in agreement with experimental observations.

The presence of micro-bubbles resulting from nucleate boiling was found to be particularly difficult to reproduce. Due to the size of the bubbles, a high level of spatial refinement was required for this phenomenon to be captured accurately. Furthermore, the model was found to have a tendency over-estimate the spreading dynamics of the droplet. This could be caused by the use of a constant parameter for the contact angle, which currently is still assumed to be solely a function of the temperature at the solid-liquid contact line. Accurate reproduction of the experimental results, therefore, is expected to require the effects of fluid velocity (advancing and receding) on the contact angle parameter to be characterised properly. Systematic errors resulting from the use of axisymmetric boundary condition was also expected to contribute towards this discrepancy.

REFERENCES

BERRY, T., McKEEN, T., PUGSLEY, T., and DALAI, A. (2004), "Two-dimensional reaction engineering model of the riser section of a fluid catalytic cracking unit", *Ind. Eng. Chem. Res.*, **43**, 5571-5581.

CHANDRA, S. and AVEDISIAN, C.T., (1991), "On the collision of a droplet with a solid surface", *Proc. R. Soc. Lond. A*, **432**, 13-41.

HARDT, S. and WONDRA, F. (2008), "Evaporation model for interfacial flows based on a continuum-field representation of the source terms", *J. Comput. Phys.* **227**, 5871-5895.

KUNKELMANN, C. and STEPHAN, P. (2010), "Modification and extension of a standard volume-of-fluid solver for simulating boiling heat transfer", *V European Conference on Computational Fluid Dynamics, ECCOMAS CFD 2010*, Pereira, J. C. F., Sequira, A. (eds.), Lisbon, Portugal.

NAYAK, S.V., SAKET, L.J., and RANADE, V.V. (2005), "Modeling of vaporization and cracking of liquid oil injected in a gas-solid riser", *Chem. Eng. Sci.*, **60**, 6049-6066.

OpenFOAM Project web pages, http://www.openfoam.org, viewed 31 August 2012.

SAZHIN, S.S. (2006), "Advanced models of fuel droplet heating and evaporation", *Prog. Energy Combust. Sci.*, **32**, 162-214.

SUSSMAN, M. and PUCKETT, E.G. (2000), "A coupled level set and volume-of-fluid method for computing 3d and axisymmetric incompressible two-phase flows", *J. Comput. Phys.* **162**, 301-337.

